Universal Features of Shape Transitions in Hot Rotating Nuclei

Y. Alhassid
A. W. Wright Nuclear Structure Laboratory, Yale University, New Haven, Connecticut 06511

S. Levit
Center for Theoretical Physics, Department of Physics, Laboratory of Nuclear Science, Massachusetts Institute of Technology, Cambridge, Massachusetts 02139, and Department of Nuclear Physics, The Weizmann Institute of Science, Rehovot 76100, Israel[a]

and

J. Zingman[b]
A. W. Wright Nuclear Structure Laboratory, Yale University, New Haven, Connecticut 06511
(Received 20 March 1986)

The Landau theory of shape transitions in hot rotating nuclei is introduced and the universal features of such transitions are derived. The phase diagram of the excitation energy versus angular momentum J for nuclei with prolate ground states shows a transition line from triaxial to oblate shapes. The transition is first order for small values of J and becomes second order above a certain value which is the analog of the tricritical point. Nuclear shapes change very rapidly from near prolate to oblate in the vicinity of this point. The theory is used to calculate the phase diagram of the ^{166}Er nucleus.

PACS numbers: 21.60.−n, 05.70.Fh, 24.60.Dr

Growing experimental information is presently becoming available on the equilibrium shapes of highly excited nuclei formed in heavy-ion reactions.[1,2] The energy E^* dissipated in such reactions is usually accompanied by an angular momentum transfer J. Thus E^* and J or their intensive partners—the temperature T and the angular velocity ω—are the relevant macroscopic parameters controlling the shape of the hot rotating nucleus.

The high level density of hot nuclei warrants a statistical treatment. The theoretical analysis of nuclear shape transitions is usually based on some version of a finite-temperature mean-field description, e.g., the shell-correction Strutinsky procedure[3] or the thermal Hartree-Fock approximation,[4] etc., in which a trial free energy at a given T and ω is minimized. In this Letter we introduce a unified framework based on the Landau theory of phase transitions[5] in which the most relevant and universal results of any microscopic mean-field theory of nuclear shape transitions at finite T and ω can be incorporated. The framework offers a useful and economical parametrization of the results of microscopic calculations and singles out a small number of combinations of the parameters upon which the behavior of the equilibrium shape depends. Below we summarize the main results of the approach; for details cf. Alhassid, Levit, and Zingman.[6]

The trial free energy of the rotating nucleus in a mean-field theory is a function of the single-particle density matrix ρ, $F=F(T,\omega,\rho)$. Out of the infinitely many variational parameters represented by ρ the most crucial for the description of shape transitions are the quadrupole deformation parameters $\alpha_{2\mu}$, so that F can be reduced (cf. Levit and Alhassid[7]) to a function $F(T,\omega,\alpha_{2\mu})$. $\alpha_{2\mu}$ here represent, e.g., the average quadrupole moment in the Hartree-Fock approach or the shape parameters of the potential in the Strutinsky calculations, etc.

The dependence of F on $\alpha_{2\mu}$ can be determined from symmetry considerations by use of rotational invariance. It is convenient to let ω be a vector along an arbitrary direction in space. The free energy $F=\langle H\rangle - TS-\boldsymbol{\omega}\cdot\langle \mathbf{J}\rangle$ is then $F=F(T,\boldsymbol{\omega},\alpha_{2\mu})$ and in the terminology of the Landau theory describes a statistical system with a quadrupole order parameter in a vector field $\boldsymbol{\omega}$.

F is a scalar and can depend only upon invariant quantities constructed out of $\alpha_{2\mu}$ and $\boldsymbol{\omega}$. The ω-independent invariants are the standard $[\alpha\times\alpha]^{(0)}\sim\beta^2$ and $[(\alpha\times\alpha)^{(2)}\times\alpha]^{(0)}\approx\beta^3\cos3\gamma$, where β and γ are the Hill-Wheeler parameters in the intrinsic frame. The lowest ω-dependent invariants are second order in ω, e.g., $[\omega\times\omega]^{(0)}$, $[(\omega\times\omega)^{(2)}\times\alpha]^{(0)}$, $[(\omega\times\omega)^{(2)}\times(\alpha\times\alpha)^{(2)}]^{(0)}$. Assuming the analyticity of F and small ω we write in Cartesian coordinates

$$F(T,\boldsymbol{\omega},\alpha)=F(T,\omega=0,\alpha)-\frac{1}{2}\sum_{i,j=1}^{3}I_{ij}(T,\alpha)\omega_i\omega_j, \tag{1}$$

where I_{ij} is the moment of inertia tensor built from the α. Its general form to second order in α is

$$I_{ij}=\delta_{ij}\{I_0(T)+I_1(T)(\alpha\times\alpha)^{(0)}\}+\{R(T)\alpha+D(T)(\alpha\times\alpha)^{(2)}\}_{ij}. \tag{2}$$

The first term on the right-hand side of (1), the free energy at $\omega = 0$, can be written to fourth order in α as

$$F(T, \omega = 0, \alpha_{2\mu}) = F_0(T) + A(T)\beta^2 - B(T)\beta^3 \cos 3\gamma + C(T)\beta^4. \quad (3)$$

The general temperature dependence of the coefficients A, B, and C (F_0 is irrelevant in the minimization) was investigated in Ref. 7 with the following results. For stability one must require $C(T) > 0$ and nuclei with deformed ground state must have $A(T) < 0$ at low temperatures. The prolate-oblate asymmetry requires $B(T) \neq 0$. For definiteness we will discuss the more frequently occuring prolate case $B(T) > 0$. When T increases $A(T)$ changes sign at some $T = T_c$ which is usually between 1 and 2 MeV. The topography of the free-energy surface given by (3) is controlled[7] by the dimensionless combination

$$\tau = AC/B^2 \quad (4)$$

which is monotonic in $T - T_c$ in the vicinity of T_c.

The free energy (1) depends on β, γ, and the orientation angles Ω relative to the rotation axis $\boldsymbol{\omega}$. Minimizing with respect to Ω one finds that the principal axis with the largest moment of inertia must be parallel to $\boldsymbol{\omega}$. In order to facilitate this condition it is convenient to call that axis z, define β and γ with respect to this axis, and let γ vary over the entire plane, $-180° \leq \gamma \leq 180°$. With this convection $\gamma = 0°$ and $\gamma = -180°$ describe, respectively, prolate and oblate shapes rotating around their symmetry axes while $\gamma = \pm 120°$ and $\gamma = \pm 60°$ represent, respectively, prolate and oblate shapes rotating perpendicular to their symmetry axes. Minimizing F in the entire β-γ plane one should select only those minima which have moments of inertia obeying the condition $I_{zz} > I_{xx}, I_{yy}$, i.e., with the largest I along $\boldsymbol{\omega}$. We emphasize that our choice of $\boldsymbol{\omega}$ parallel to z is different from the standard (where $\boldsymbol{\omega}$ is parallel to x). Thus a shape β, γ in our convention is described by β, $-(\gamma + 120°)$ in the standard one. We note that the calculational advantages in the present case are overwhelmingly for this change of the convention.[6] With $\boldsymbol{\omega}$ parallel to z expressions (1)–(3) give

$$F(T, \omega, \alpha_{2\mu}) = F_0(T) + A(T)\beta^2 - B(T)\beta^3 \cos 3\gamma + C(T)\beta^4 - \tfrac{1}{2} I_{zz}(\beta, \gamma, T)\omega^2, \quad (5)$$

where

$$I_{zz} = I_0(T) - 2R(T)\beta \cos\gamma + 2I_1(T)\beta^2 + 2D(T)\beta^2 \sin^2\gamma \quad (6)$$

with I_1, R, and D redefined to absorb various numerical constants. The R term here has the leading shape dependence of the rigid-body moment of inertia while the D term alone would represent the leading irrotational moment of inertia. In generic nuclear situations R is not zero and the lowest-order term, $-2R\beta\cos\gamma$, plays a dominant role. The term $2I_1\beta^2$ can be combined with $A\beta^2$ and need not be considered separately. Below we will study the limit $D = 0$ and comment on the $D \neq 0$ case at the end.

Minimizing (5) one finds that at negative values of τ, Eq. (4), i.e., at low T and not too large ω, there are seven extrema of (5) in the entire (β, γ) plane which are located symmetrically according to the $\gamma \rightarrow -\gamma$ invariance of (5). When $D = 0$ the condition $I_{zz} > I_{xx}, I_{yy}$ selects those extrema which fall into the sector $|\gamma| \geq 120°$ only. At negative τ there are three such extrema, one oblate ($\gamma = -180°$) and two triaxial related by the $\gamma \rightarrow -\gamma$ symmetry. Only one of the latter should be considered since they both give the same shape up to a rotation by 90° around the z axis. We choose to work in the sector $-180° \leq \gamma \leq -120°$. For $B > 0$ in (5) and $\tau < 0$ the triaxial extremum is the stable equilibrium shape while the oblate is a saddle point.

Letting τ now increase towards positive values for fixed ω one finds crucial differences depending on whether ω is smaller or larger than

$$\omega_c = \tfrac{9}{16}(B/C)(B/R)^{1/2}. \quad (7)$$

For fixed $\omega/\omega_c > 1$ and τ increasing the triaxial minimum moves towards the oblate saddle point and coincides with it when τ reaches

$$\tau = \tfrac{9}{8}[1 - (\omega/4\omega_c - 1)^2]. \quad (8)$$

When τ increases beyond (8) the oblate shape becomes and remains the only stable minimum. We show this on the right-hand side of Fig. 1. Recalling the the $\gamma \rightarrow -\gamma$ symmetry one finds that the topography of F, Eq. (5) when τ crosses (8) is typical of second-order transitions where two equally deep symmetry-related minima coalesce with the third extremum—the saddle point.

When $\omega/\omega_c < 1$ the initial location of extrema at low τ is similar to the case $\omega/\omega_c > 1$. When τ reaches (8) the oblate saddle point turns into a local minimum but the triaxial minimum is still separated from it. Instead when τ increases past (8) a new triaxial saddle point emerges out of the oblate and moves towards the old. The two coalesce and disappear when τ reaches

$$\tau = \tfrac{9}{32}(1 + \tfrac{3}{4}\omega^2/\omega_c^2). \quad (9)$$

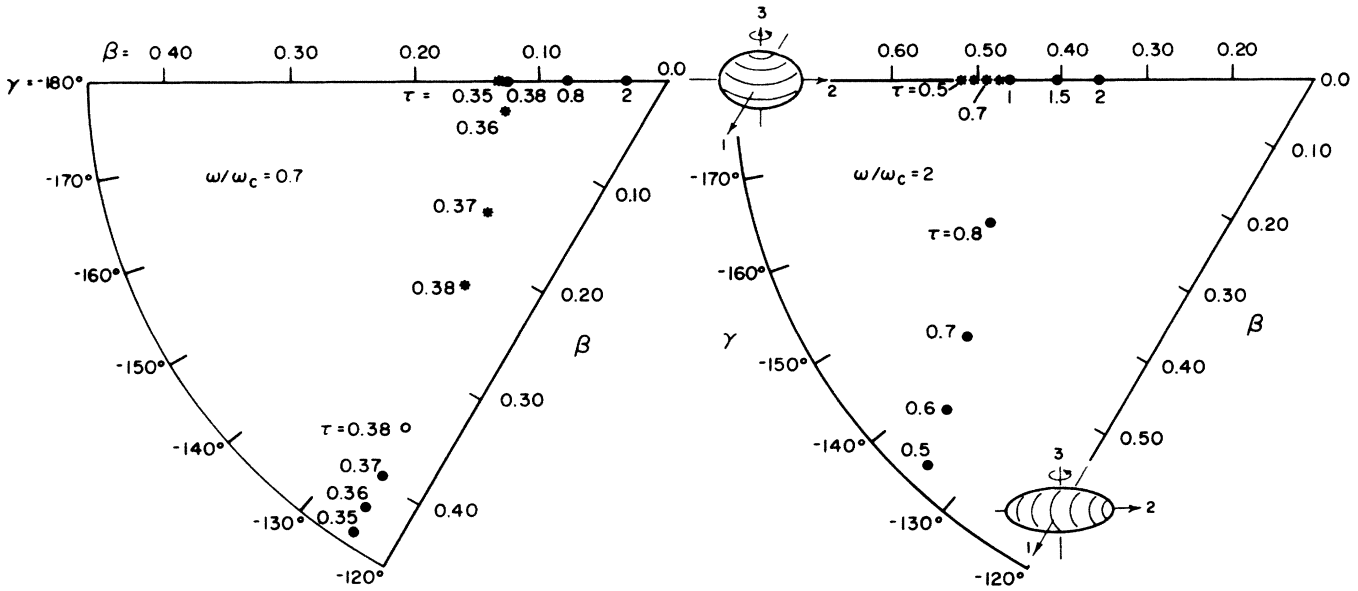

FIG. 1. Motion of the saddle points in the β-γ plane with changing τ and fixed ω/ω_c. The z axis is parallel to $\boldsymbol{\omega}$ and β is measured in units of B/C. On the right a second-order transition is shown for $\omega/\omega_c = 2$ with dots denoting a global minimum and asterisks a saddle point. On the left a first-order transition is shown for $\omega/\omega_c = 0.7$ where notation is as on the right but in addition open dots denote a local minimum.

Above (9) only the oblate minimum remains. This motion of extrema is shown on the left-hand side of Fig. 1. Obviously (8) and (9) define the boundaries of a "coexistence" region where both triaxial and oblate shapes are local minima. At a certain value of τ in between (8) and (9) the free energies of the two minima become equal and the global minimum shifts discontinuously from triaxial to oblate in the way typical of the first-order transitions. The value of τ at which this happens is given by a complicated expression[6] which we do not record here. It

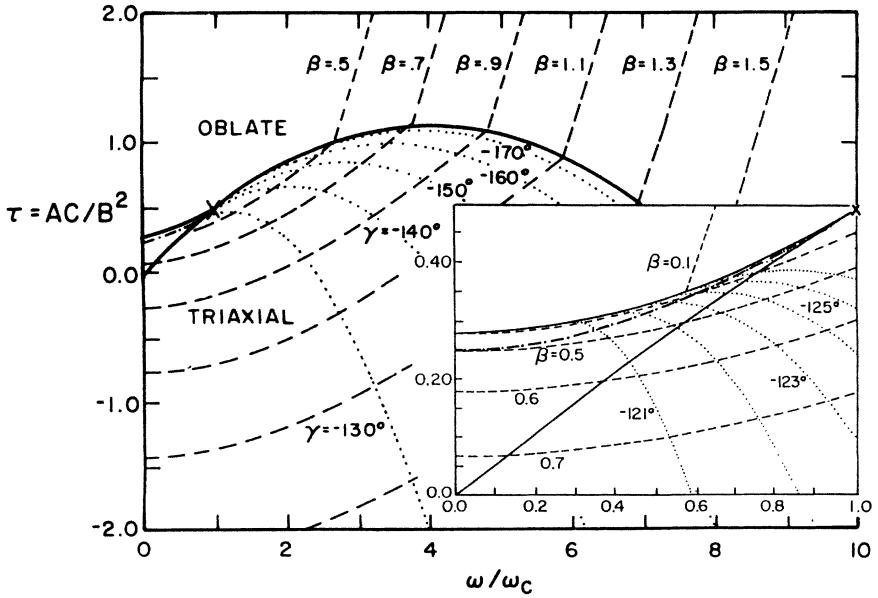

FIG. 2. Phase diagram in variables τ and ω/ω_c. The tricritcal point (at $\omega/\omega_c = 1$) is denoted by a cross. To its left is the first-order transition line (dash-dotted) and to its right is the second-order transition line (solid). The other two solid lines, to the left, are the stability limits of the triaxial and oblate phases. Also shown are β and γ contour lines where β is measured in units of B/C. Inset: The first-order transition region.

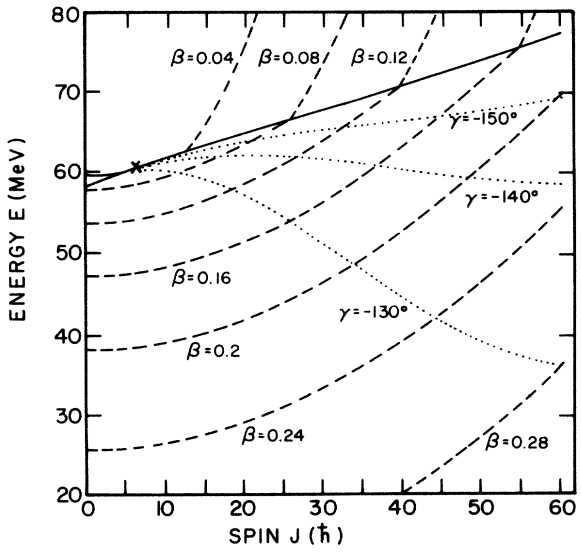

FIG. 3. Phase diagram in variables E^*, J for ^{166}Er. Lines as in Fig. 2. On and above the second-order transition line the shape is oblate ($\gamma = -180°$).

goes to $\tau = \frac{1}{4}$ for $\omega \to 0$. Note that when $B(T)$ is small near the transition temperature the above transition is almost continuous as in the example of Ref. 7.

The above results are summarized on the phase diagram, Fig. 2, with the lines of constant equilibrium β and γ drawn in. The solid line for $\omega/\omega_c > 1$ is the line (8) of second-order transitions and separates the triaxial "phase" below from the oblate phase above. For $\omega/\omega_c < 1$ the two solid lines denote Eqs. (8) and (9) which define the coexistence region and give the lower boundary of the oblate phase and the upper boundary of the triaxial phase, respectively. The dash-dotted line denotes the first-order transitions. It meets the second-order line at $\omega = \omega_c$ and $\tau = \tau_c = \frac{63}{128}$. Phase diagrams similar to Fig. 2 are observed in, e.g., liquid crystals and antiferromagnets.[8,9] There the point similar to our $\omega = \omega_c$, $\tau = \tau_c$ is known as the tricritical point.

In finite nuclear systems it is probably difficult to observe the order of the transition. More important is the rapid change from almost prolate to oblate shape in the vicinity of the tricritical point, clearly seen from the behavior of the lines of constant γ in Fig. 2.

The phase diagram in the variables τ and ω/ω_c has universal character. However, the precise dependence of τ and ω on the experimentally accessible E^* and J is not universal and must be studied in the context of particular nuclei. We demonstrate such a study for ^{166}Er. We found the functions $A(T)$, $B(T)$, and $C(T)$ by fitting the form (3) to the free-energy surfaces at $\omega = 0$ calculated by a finite-temperature Strutinsky procedure. For the ω-dependent terms in (5) we assumed the rigid-body moment of inertia setting $I_0 = 2mR_0^2/5$, $R = (5/16\pi I_0)^{1/2}$, and $D = I_1 = 0$. Relating T and ω to E^* and J, we have constructed the phase diagram shown in Fig. 3. The angular momentum of the tricritical point is $J_c \cong 7\hbar$ and its temperature is $T_c \cong 1.7$ MeV. In the region $J \simeq 10$–$20\hbar$, $E^* \simeq 60$ MeV, where ^{166}Er was recently studied experimentally[1,2] the shape is very sensitive to the values of E^* and J offering a possible explanation of the observed rapid transition from almost prolate to an oblate shape.

Our calculations for ^{166}Er can be further improved by use of more elaborate mean-field schemes. It appears, however, that at the present stage the qualitative framework presented above should be sufficient to stimulate more experimental studies.

The generalization of our analysis to the case $D \neq 0$ is straightforward. The qualitative behavior is similar to the case $D = 0$ but there are important quantitative differences in the large-ω region (cf. Ref. 6).

This work was partly supported by the Department of Energy under Contracts No. DE-AC02-76-ER-03074 and No. DE-AC02-76-ER-03069. One of us (S.L.) acknowledges the hospitality of the Center for Theoretical Physics at Massachusetts Institute of Technology and the Wright Nuclear Structure Laboratory at Yale University. Another of us (Y.A.) acknowledges the hospitality of the Center for Theoretical Physics, at Massachusetts Institute of Technology. We thank J. Manoyan for his help in the Strutinsky calculations of ^{166}Er. One of us (Y.A.) is an Alfred P. Sloan Fellow.

[a] Permanent address.

[b] Present address: Lawrence Livermore National Laboratory, Livermore, CA 94550.

[1] C. A. Gossett, K. A. Snover, J. A. Behr, G. Feldman, and J. L. Osborne, Phys. Rev. Lett. **54**, 1486 (1985).

[2] J. J. Gaardhøje, C. Ellegaard, B. Herskind, and S. G. Steadman, Phys. Rev. Lett. **53** 148 (1984).

[3] A. K. Ignatiuk, I. N. Mikhailov, L. H. Molina, R. G. Nazmitdinov, and K. Pomorsky, Nucl. Phys. **A346**, 191 (1980).

[4] P. Quentin and M. Flocard, Ann. Rev. Nucl. Sci. **28**, 523 (1978).

[5] L. D. Landau and E. M. Lifshitz, *Statistical Physics* (Pergamon, New York, 1970), Sect. 139.

[6] Y. Alhassid, S. Levit, and J. Zingman, to be published.

[7] S. Levit and Y. Alhassid, Nucl. Phys. **A413**, 439 (1984).

[8] A. Aharony, in *Critical Phenomena,* edited by F. J. W. Hahne, Lecture Notes in Physics Vol. 186 (Springer-Verlag, New York, 1983), p. 207.

[9] R. N. Hornreich, Phys. Lett. **109A**, 232 (1985).